CLC_____ Number___

UDC_____ Available for reference ☐ Yes ☐

No

Undergraduate Thesis

Thesis Title: Large-eddy Simulation with Wall Model in Lattice Boltzmann Method for Turbulent Channel Flow

Student Name: Weixuan Li

Student ID: 11912635

Department: Mechanical and Aerospace Engineering

Program: Theoretical and Applied Mechanics

Thesis Advisor: Lian-ping Wang

Date: 2023.5.7

Letter of Commitment for Integrity

1. I solemnly promise that the paper presented comes from my independent research work under my supervisor's supervision. All statistics and images are real and reliable.

2. Except for the annotated reference, the paper contents no other published work or achievement by person or group. All people making important contributions to the study of the paper have been indicated clearly in the paper.

3. I promise that I did not plagiarize other people's research achievement or forge related data in the process of designing topic and research content.

4. If there is violation of any intellectual property right, I will take legal responsibility myself.

Signature: 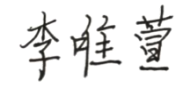

Date: 2023.5.7

Large-eddy Simulation with Wall Model in Lattice Boltzmann Method for Turbulent Channel Flow

Weixuan Li

(Department of Mechanical and Aerospace Engineering, Supervisor: Lian-ping Wang)

[Abstract]: Turbulent flows are relevant to a wide range of engineering applications and natural phenomena. Accurate prediction of these flows is essential for optimizing the design and performance of various engineering systems. This study investigates the performance of Large-eddy Simulation (LES) with a wall model in the lattice Boltzmann Method (LBM) for simulating turbulent channel flow. This study builds upon previous research on LES and wall models in LBM, implementing the Smagorinsky sub-grid scale model and the Musker wall model to an original direct numerical simulation (DNS) code using LBM. The accuracy and applicability of the approach are assessed by comparing the LES results to DNS data and those obtained by other researchers reported in the literature simulating the turbulent channel flow with friction Reynolds number at $Re_\tau = 180$. The study focuses on the statistical data obtained during the stationary stage of the turbulent flow, which provides crucial insights into turbulent structures and statistics. The mean flow streamwise velocity profiles, mean turbulent Reynolds stress profiles, mean root-mean-square velocity profiles, the normal gradient of the streamwise velocity, and the normalized turbulent viscosity profiles are analyzed and compared. The results reveal excellent agreement between

the LES and DNS methods, as well as with the published data. The LES profile fits well with the standard viscous sublayer profile and the logarithmic inertial layer profile from the canonical boundary layer theory. The LES method effectively captures the average velocity profile in the viscous sublayer and the logarithmic layer while maintaining accuracy and avoiding kink in the logarithmic law's gradient. Furthermore, the LES results fit well with the DNS method and the published data for the turbulent Reynolds stress profiles and the mean root-mean-square velocity profiles. The insights gained from this study contribute to the advancement of LES methods and LBM, improve the understanding of turbulent structures and wall-bounded turbulent flows and benefit further advancements in computational fluid dynamics.

[Keywords]: turbulent channel flow; lattice Boltzmann equation; large-eddy simulation; wall model

大涡模拟与壁面模型在格子玻尔兹曼方法模拟湍流槽道流应用中的方法研究

李唯萱

（力学与航空航天系　指导教师：王连平）

[摘要]：湍流广泛存在于工程应用和自然现象中。准确预测湍流流动对于优化各种工程系统的设计和性能至关重要。本研究在格子玻尔兹曼方法（LBM）对湍流进行直接数值模拟的基础上，结合大涡模拟（LES）与壁面模型，探讨湍流槽道流的大涡模拟方法的性能。本研究将 Smagorinsky 亚格子模型和 Musker 壁面模型应用于 LBM 的直接数值模拟。通过将 LES 结果与摩擦雷诺数同为 180 的直接数值模拟（DNS）数据以及文献中其他研究者的数据进行比较，评估了该方法的准确性和适用性。本研究关注湍流流动稳态过程中获得的统计数据，这些数据为理解湍流结构和统计量提供了关键依据。本研究分析并比较了平均流动方向速度剖面、平均湍流雷诺应力剖面、平均均方根速度剖面、流向速度的垂直壁面梯度以及湍流粘度剖面。结果表明，LES 与 DNS 方法以及文献中的湍流槽道流模拟数据之间具有较好的一致性。本研究的成果有助于推进 LBM 与 LES 方法的发展，提高对湍流结构和壁面湍流流动的理解，有助于计算流体力学的进一步发展。

[关键词]：湍流槽道流；格子玻尔兹曼方法；大涡模拟；壁面模型

Table of Contents

1. Introduction 1

2. Methods 4

2.1 The lattice Boltzmann method 4

2.2 The large-eddy simulation 6

2.3 Boundary conditions and the wall model 7

3. Numerical case set up 9

4. Results 10

5. Conclusions 17

References 19

Acknowledgement 21

1. Introduction

Turbulent flows are ubiquitous in many engineering applications and natural phenomena, ranging from the flow in pipes and channels to the motion of air around aircrafts and wind turbines. The accurate prediction of turbulent flows is essential for optimizing the design and performance of various engineering systems.

The most common used method, direct numerical simulation (DNS), can produce data of extremely high accuracy, but its computational cost makes the simulations for turbulent flows at high Reynolds numbers infeasible. For a statistically homogeneous and isotropic turbulent flow, the span of turbulence length scales from the largest scale L to the smallest eddy length scale η is proportional to $Re^{\frac{3}{4}}$, which means that we need to use $O(Re^{\frac{9}{4}})$ degrees of freedom to represent all the scales in a volume of edge L. In addition, in order to trace the evolution of the solution within a volume of edge length L over a duration that aligns with the characteristic time of the highest energy scale, we are required to conduct numerical computations on the Navier-Stokes equations $O(Re^3)$ times[1].

There are many methods to reduce the resolutions used in the numerical simulation. For example, the Reynolds Averaged Navier-Stokes (RANS) simulation only calculates the time average of the solution of turbulent flows directly[2]. Some methods, including Unsteady Reynolds Averaged Navier-Stokes (URANS) Simulation, Semi-Deterministic Simulation, and Coherent Structure Capturing calculate directly only certain low-frequency modes in the average time and space field[3,4]. Large-eddy Simulation (LES) is a numerical technique used to simulate turbulent flows by resolving large-scale turbulent structures only while modeling the smaller, unresolved scales. It is the method that is discussed and used to simulate turbulent flows in this thesis.

Joseph Smagorinsky first introduced the concept of LES to simulate atmospheric air currents[5], which was later applied to turbulent channel flows by Deardorff J W[6].

Many Sub-grid scale (SGS) models have been developed and used for modeling the unresolved scales. The first SGS model was developed by Joseph Smagorinsky, which is called the Smagorinsky-Lilly SGS model[5]. Germano et al. proposed the dynamic model to reduce the excess numerical dissipation of the Smagorinsky model[7]. The Lagrangian dynamic model proposed by Meveneau et al., is another effective way to improve the eddy viscosity coefficient. This method average over the characteristic Lagrangian time scale, so that the model is purely dissipative, guaranteeing numerical stability when coupled with the Smagorinsky model[8]. Schumann U proposed a turbulent kinetic energy model, which features a two-part SGS stress model to account for locally isotropic turbulence and inhomogeneous effects, while incorporating integral conservation equations in the finite difference procedure[9].

Because of the small characteristic length and the high anisotropy of the flow field near the wall, different kinds of wall models which can reduce the number of required grid points greatly were proposed, to be combined with LES. The wall stress models provide the values of wall stresses and the values of the wall-normal velocity components, where the near-wall events are averaged over the first grid cell. It is the model we mainly consider and discuss. Musker A J introduced a clear equation for the mean velocity distribution across a smooth surface, fulfilling both the continuity and momentum equations in proximity to the wall[10]. Schumann U devised a wall model for planar channel flow propelled by a known pressure gradient, necessitating that the mean velocity field adheres to the logarithmic law[11]. Base on this model, Grötzbach G proposed an extended model which does not need to specify the mean wall shear stress, also allowing variations of the total mass flux through the channel[12]. The wall model provides a new boundary condition as a substitute for traditional non-slip boundary conditions for the LES. This approach, with its ability to significantly reduce the number of required grid points and provide accurate wall stresses and wall-normal velocity values, is commonly used to deal with the highly heterogeneous and anisotropic flows near the wall of turbulent channel flows.

In recent years, the lattice Boltzmann Method (LBM) has gained popularity as an

alternative to traditional Navier-Stokes solvers due to its simplicity, ease of implementation, and suitability for parallel processing. Shan et al. presented the theoretical framework of LBM, which systematically discretizes the Boltzmann kinetic equation, providing a clear and rigorous procedure for obtaining higher-order approximations and revealing macroscopic moment equations that give rise to Navier-Stokes hydrodynamics and beyond, proving the benefits of LBM for complex and micro-scale flows[13]. Furthermore, Frapolli at al. presents an advanced LBM that overcomes the low Mach number limitation by incorporating a multispeed lattice, accurate equilibrium evaluation, and entropic relaxation for the collision, thus extending the method's applicability to a wide range of fluid flows, including transonic and supersonic scenarios, as demonstrated through simulations of bow shocks and decaying compressible turbulence with shocklets[14]. Moreover, Wang et al. demonstrates the application of LBM in simulating both single-phase turbulent channel flow and particle-laden flows, showcasing the versatility of the method while obtaining excellent agreement with published data and other numerical methods such as the Chebychev-spectral method and finite difference method with direct forcing, further highlighting the efficacy of LBM in handling complex fluid-particle interactions in turbulent environments[15].

The combination of LES with wall models in LBM has also been studied recently. Maeyama et al. developed a wall-modeled large-eddy simulation (WMLES) based on LBM in 2021, incorporating an Image-Point method and a strategy for determining the turbulent eddy viscosity profile near the wall, demonstrating robustness and accuracy in simulating turbulent channel flows on non-body-fitted Cartesian grids[16]. Another study successfully employed a three-dimensional filter-matrix lattice Boltzmann (FMLB) model based on LES, incorporating the Vreman subgrid-scale eddy-viscosity model for accurate near-wall predictions, with the obtained turbulence statistics showing strong agreement with the LES results of a multiple-relaxation-time (MRT) LB model and DNS data, demonstrating the model's reliability and accuracy in simulating wall-bounded turbulent flows[17]. These studies

showcase the potential and effectiveness of combining LES with wall models in LBM, providing reliable and accurate simulations for wall-bounded turbulent flows, making it a promising approach for various engineering applications.

This study builds upon the literature on LES with wall models in LBM. The primary goal of this work is to investigate the performance of LES with a wall model in the LBM for simulating turbulent channel flow. This thesis will implement the Smagorinsky sub-grid scale model and the Musker wall model to the original direct numerical simulation code using the lattice Boltzmann Method, to assess the accuracy and applicability of this new approach by comparing the LES results to the DNS data and those obtained by other researchers reported in the literature simulating turbulent channel flow with the friction Reynolds number at $Re_\tau = 180$. The insights gained from this work will contribute to the advancement of LES methods in LBM and help improve the understandings and predictions of turbulent channel flows.

2. Methods

2.1 The lattice Boltzmann method

In this study, our numerical method is developed based on an original direct numerical simulation code that uses the lattice Boltzmann method. The lattice Boltzmann method discretizes the continuous Boltzmann equation to a set of the distribution functions. The distribution function can only move in certain directions and collide with each other on the grid points. For the collision operator, the Bhatnagar-Gross-Krook model, which assumes that the particle distribution function relaxes to its equilibrium state at a constant rate, is used to simulate the turbulent channel flow[18]. The lattice Boltzmann equation with the external force using the BGK model[18,19] can be written as

$$f_i(\boldsymbol{x} + \boldsymbol{c_i}\Delta t, t + \Delta t) = f_i(\boldsymbol{x}, t) - \frac{1}{\tau}(f_i(\boldsymbol{x}, t) - f_i^{eq}(\boldsymbol{x}, t)) + F_i(\boldsymbol{x}, t)\Delta t \qquad (1)$$

where $f_i(x,t)$ is the distribution function, c_i is the microscopic velocity, τ is the relaxation time, f_i^{eq} is the equilibrium distribution function, Δt is the lattice time step and F_i is the forcing term. The D3Q19 model (three space dimensions and 19 discrete velocities) is used and given as

$$c_i = \begin{cases} (0,0,0) \ \ i = 0, \\ (\pm 1,0,0), (0,\pm 1,0), (0,0,\pm 1) \ \ i = 1\sim 6 \\ (\pm 1,\pm 1,0), (\pm 1,0,\pm 1), (0,\pm 1,\pm 1) \ \ i = 7\sim 18 \end{cases} \tag{2}$$

The relation between the relaxation time in Eq. 1 and the molecular viscosity of the fluid can be described as

$$\tau = \frac{1}{2} + \frac{\nu}{{c_s}^2 \Delta t} \tag{3}$$

where c_s is the sound speed with the value of $\frac{1}{\sqrt{3}}$ in the lattice unit. The equilibrium distribution function and the external forcing term are given by

$$f_i^{eq} = \rho\omega_i \left(1 + \frac{3\boldsymbol{c_i}\cdot\boldsymbol{u}}{{c_s}^2} + \frac{9(\boldsymbol{c_i}\cdot\boldsymbol{u})^2}{2{c_s}^4} - \frac{3\boldsymbol{u}^2}{2{c_s}^2}\right) \tag{4}$$

$$F_i = \rho\omega_i \left(1 - \frac{1}{2\tau}\right)\left[\frac{\boldsymbol{c_i} - \boldsymbol{u}}{{c_s}^2} + \frac{(\boldsymbol{c_i}\cdot\boldsymbol{u})}{{c_s}^4}\boldsymbol{c_i}\right]\cdot\boldsymbol{g} \tag{5}$$

where ω_i is the lattice weight, $\boldsymbol{g}$ is the external body acceleration vector, $\boldsymbol{u}$ is the macroscopic velocity vector, ρ is the macroscopic density.

Through the Chapman-Enskog expansion, the lattice Boltzmann equation can be transformed into the nearly incompressible Navier-Stokes equations. Macroscopic properties, such as density, momentum, and pressure, can be acquired by integrating the zeroth to second-order moments of the distribution function. In the discrete form, the integration[20] can be described as

$$\rho = \sum_{i=0}^{18} f_i \tag{6}$$

$$\rho \boldsymbol{u} = \sum_{i=0}^{18} (\boldsymbol{c_i} f_i) + \frac{1}{2}\rho \boldsymbol{g} \Delta t \tag{7}$$

$$\boldsymbol{P} = \sum_{i=0}^{18} (\boldsymbol{c_i} - \boldsymbol{u})(\boldsymbol{c_i} - \boldsymbol{u}) f_i \tag{8}$$

The simulation procedure of LBM of each iteration contains two steps: the collision step and the streaming step, where the distribution function can only be solved in the collision step at the fluid lattice nodes.

2.2 The large-eddy simulation

Large-eddy simulation is a simulation method that captures only the large-scale turbulent fluctuations and uses sub-grid-scale models to represent the effects of small-scale eddies. One of the most critical elements of this method is the closure of the viscosity term in the equations. Besides the molecular viscosity, this method adds a term, the turbulent viscosity ν_t, to represent the effects of small-scale eddies. The Smagorinsky model is used to model the non-resolved scales[5], which can be described as

$$\nu_t = (C\Delta)^2 \sqrt{2\widetilde{S_{ij}}\widetilde{S_{ij}}} \tag{9}$$

where $\Delta = \delta x$ is the lattice spacing, and C is a model constant. Note that $C = C_s^2$, where C_s is the constant and we pick the value of $C_s = 0.12$ from its relation with the Kolmogorov constant[21]. Then, the molecular viscosity ν in the governing equation of the direct numerical simulation can be replaced by the effective viscosity ν_{eff}

$$\nu_{eff} = \nu + \nu_t \tag{10}$$

The strain rate of the filtered velocity field $\widetilde{S_{ij}} = \frac{1}{2}(\frac{\partial \widetilde{u_i}}{\partial x_j} + \frac{\partial \widetilde{u_j}}{\partial x_i})$, where u_i is a velocity component of the macroscopic velocity tensor, and x_i is a space direction component in the Cartesian coordinate system. The magnitude of the filtered strain rate can be computed directly from the non-equilibrium distribution[22], as

$$|\tilde{\mathbf{S}}| = \sqrt{2\widetilde{S_{ij}}\widetilde{S_{ij}}} = \frac{1}{2\rho c_s^2 \tau_{eff} dt}\sqrt{2\widetilde{\pi}_{ij}^{neq}\widetilde{\pi}_{ij}^{neq}}, \widetilde{\pi}_{ij}^{neq} = \sum_{\alpha=0}^{18}(f_{LBM} - f^{eq})c_i c_j \tag{11}$$

Therefore, the effective relaxation time is then obtained as

$$\tau_{eff} = \frac{\tau_0 + \sqrt{\tau_0^2 + 2C\Delta^2\Pi(\rho c_s^4 dt^2)^{-1}}}{2} \tag{12}$$

This effective viscosity can be used as a replacement of the molecular viscosity in the lattice Boltzmann equation using the BGK model to implement the SGS model into LBM.

2.3 Boundary conditions and the wall model

Because of the small characteristic length, the excessive dissipation of the SGS model and the high anisotropy of the flow field near the wall, the flows close to the wall are not accurately simulated by the pure SGS model of LES[1]. In this study, a near-wall function is applied, which is to build up virtual walls that maintain the mean shear stress and avoid fluids permeating, as well as capture the main structures of the near wall flows. The near-wall function can provide the average wall shear stress through which the velocity profile in the near-wall region can be produced. The

Musker wall model, with its advantage of simplicity and satisfying both the continuity and momentum equations near the wall, is chosen to provide the velocity at the first grid point. The Musker law can be described as[23]

$$u = u^* \left[5.424 arctan\left(\frac{2.0y^+ - 8.15}{16.7}\right) + 0.434 log\left(\frac{(y^+ + 10.6)^{9.6}}{((y^+)^2 - 8.15y^+ + 86.0)^2}\right) - 3.507 \right] \quad (13)$$

where u^* is the friction velocity in the streamwise direction, and $y^+ = \frac{yu^*}{\nu}$ is the position normalized by the wall unit. The relation between the friction velocity and the wall shear stress τ_w is

$$u^* = \sqrt{\frac{\tau_w}{\langle\rho\rangle}} \quad (14)$$

The Musker wall model is an implicit function with respect to the wall shear stress, and Newton method is used to solve the equation. Combined with the wall model, the van Driest damping function is adopted to correct the turbulent viscosity in the near-wall region, in order to resolve the excess dissipation problem, which is defined as[24]

$$\nu_t = \langle\rho\rangle \left[\kappa y [1 - e^{-\frac{y^+}{A^+}}]\right]^2 \left|\frac{\partial u}{\partial y}\right| \quad (15)$$

where $\langle\rho\rangle$ is the average density, κ is the von Karman constant with its value varying between 0.37 and 0.41[25], A^+ is the van Driest parameter, and $|\frac{\partial u}{\partial y}|$ is the magnitude of the streamwise velocity gradient in the normal-wall direction.

3. Numerical case set up

A 3D bi-periodic turbulent channel flow is chosen as a benchmark case to validate this LBM-LES numerical simulation method, because of a large amount of experimental data and numerical data available for this case. The sketch of the 3D turbulent channel flow case is shown in Fig. 1.

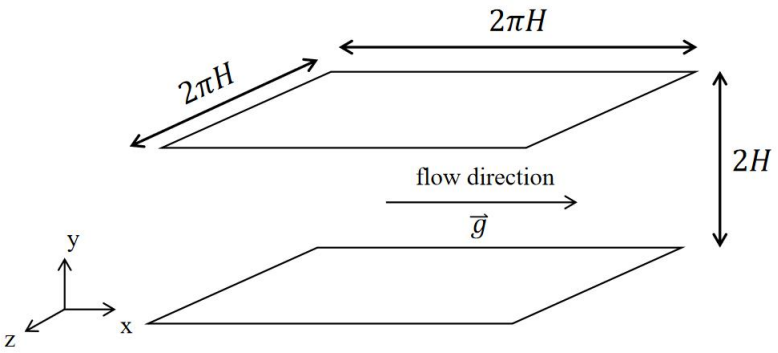

Figure 1 Sketch of the turbulent channel geomerty, with the streamwise direction (x), the transverse direction (y) and the spanwise direction (z). The half width of the channel is $H = 50$ in the lattice unit.

The x, y and z directions in the Cartesian coordinate system are chosen to represent the streamwise, the transverse and the spanwise directions of the channel flow. H is the half width of the channel, and L_x, L_z are the domain sizes in x, z directions respectively. The numerical domain size of the channel is $2\pi H \times 2H \times 2\pi H$ and the half width of the channel is $H = 50$ in the lattice unit, half of the DNS resolution. In the streamwise and the spanwise directions, the boundaries are periodic, while the non-slip boundary conditions are applied to the two channel walls. The flow is the force driven channel flow with a constant body force acting in x direction. The body force can be obtained by the force balance with the wall shear stress, as

$$2\tau_w L_x L_z = \rho g 2 H L_x L_z \tag{16}$$

$$u^* = \sqrt{Hg} \tag{17}$$

where g is the body force per unit mass. The Reynolds numbers based on the friction velocity and the mean bulk velocity are

$$Re_\tau = \frac{Hu^*}{\nu} \tag{18}$$

$$Re_m = \frac{2Hu_m}{\nu} \tag{19}$$

By using Dean correlations[26], the relation between the friction Reynolds number and the bulk Reynolds number can be described as

$$Re_m = \left(\frac{8}{0.073}\right)^{\frac{4}{7}} Re_\tau^{\frac{8}{7}} \tag{20}$$

Since the simulation method is applicable to weakly compressible flows, the Mach number has to be maintained under 0.3. The Mach number is set to be under 0.1 in this study to fulfill the weak compressibility condition, and equivalently the friction velocity is set to be $u^* = 3.5 \times 10^{-3}$. The force field used to stimulate the turbulent flows refers to Wang et al.[15], which is a non-uniform, divergence-free forcing field that can induce a rapid development of turbulence during the time period $0 < t^* < 3.24$, where $t^* = \frac{tu^*}{H}$ is the normalized time.

4. Results

Simulations are performed using both DNS and LES methods. In this section, the results from this study are presented and analyzed, where the lattice Boltzmann method and large-eddy simulation are employed to simulate wall-bounded turbulent channel flow at $Re_\tau = 180$. The results are also compared with the DNS data[27] of Moser et al. and the LES data[28] of Premnath et al. for wall-bounded turbulent channel flow at $Re_\tau = 180$ to further validate the accuracy and applicability of the

LES method.

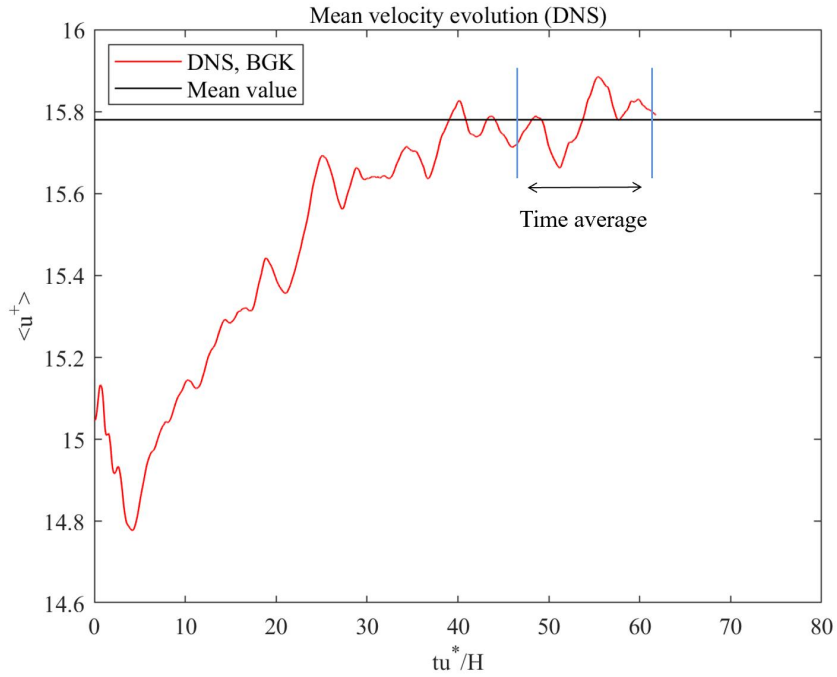

Figure 2 The evolution of the mean flow streamwise velocity as a function of normalized time of DNS. The mean velocity first decreases and then rebounds to the stationary stage with the mean velocity $15.78u^*$ after $t^* = \frac{tu^*}{H} = 38$.

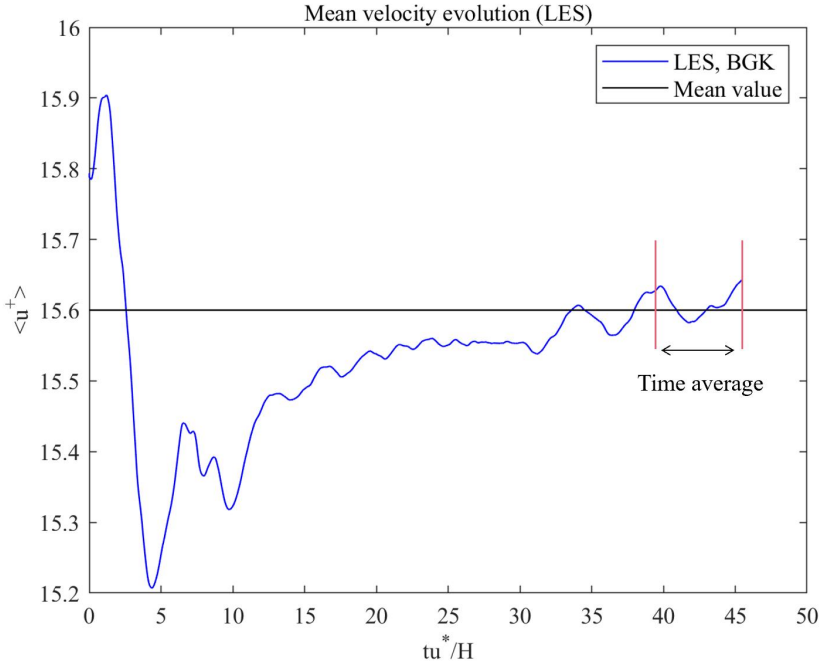

Figure 3 The evolution of the mean flow streamwise velocity as a function of normalized

time of LES. The mean velocity eventually reaches the stationary stage with the mean velocity $15.60u^*$ after $t^* = \frac{tu^*}{H} = 38$.

Fig. 2 illustrates the mean streamwise velocity as a function of normalized time for DNS, while Fig. 3 displays the mean streamwise velocity as a function of normalized time for LES. As the turbulent flow is excited ($0 < t^* < 3.24$), the mean flow velocity decreases continuously, because of the transfer of the kinetic energy from the mean flow to turbulent fluctuations. After that, the flow speed rebounds and reaches the steady state with the mean velocity $15.78u^*$ for DNS and $15.60u^*$ for LES. Both the DNS flow and the LES flow approach the stationary stage after $t^* = 38$. This study is only interested in the statistical data obtained during the stationary stage of the turbulent flow, which is important for our understandings of the turbulent structures. The average time span of the statistical data is $47 < t^* < 61$ for DNS and $38.5 < t^* < 45.5$ for LES. Moreover, the flow is homogeneous in the streamwise and the spanwise directions. Therefore, in this study, the statistical data of the properties of fluids are averaged in these two directions and only the variations in the transverse direction are concerned.

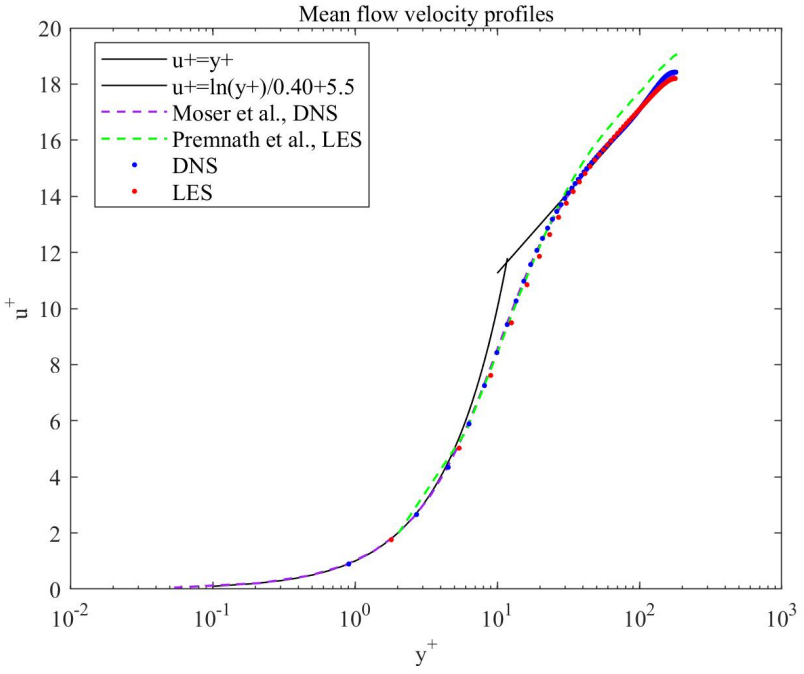

Figure 4 The log-linear mean flow velocity profiles varying in the transverse direction. The data agree well with the logarithmic law of the wall.

Fig. 4 shows the mean flow streamwise velocity profiles generated by the DNS method, LES method and from the data of Moser et al. and Premnath et al. The profiles show the variation of the normalized streamwise velocity $u^+ = {u}/{u^*}$ as a function of normalized normal distance from the wall $y^+ = {yu^*}/{\nu}$ where y^+ is the normal distance from the wall in the lattice unit. The velocity profiles are plotted in logarithmic coordinate for the distance and in linear coordinate for the velocity. The four results show excellent agreement with each other. Note that the LES data of this study agree with the DNS data better compared to the results of Premnath et al. Moreover, the LES profile fits well with the standard viscous sublayer profile ($y^+ < 5$) and the logarithmic inertial layer profile ($y^+ > 30$) from the canonical boundary layer theory. The results also show that the LES method effectively captures the average velocity profile in the logarithmic layer, maintaining accuracy and avoiding kink in the logarithmic law's gradient. This finding indicates that this LES approach does not experience issues akin to shear stress depletion, despite the wall model being implemented solely within the first cell near the wall and does not apply any treatment for the second off-wall cell.

Fig. 5 presents the mean turbulent Reynolds stress profiles normalized by u^{*2} for half of the channel. To interpret this figure, first the momentum balance equation in the x direction is introduced

$$\frac{d\langle -u_x^{'}u_y^{'}\rangle}{dy} + g + \nu\frac{d^2U}{dy^2} = 0 \tag{21}$$

Then the total stress can be described as

$$\frac{1}{u^{*2}}\left[\langle -u_x^{'}u_y^{'}\rangle + \nu\frac{dU}{dy}\right] = -\frac{y_c}{H} \tag{22}$$

where y_c is the distance of the channel center from the wall. In Eq. 22, $\frac{\langle -u_x^{'}u_y^{'}\rangle}{u^{*2}}$ represents the normalized Reynolds stress, and $\frac{1}{u^{*2}}(\nu\frac{dU}{dy})$ refers to the viscous shear stress, which is the difference between the black straight line and the data shown in Fig. 5. The LES results fit well with the DNS method and the published data. Note that the LES results show a slightly smaller maximum Reynolds stress than the DNS results, indicating larger numerical diffusion of the LES approach.

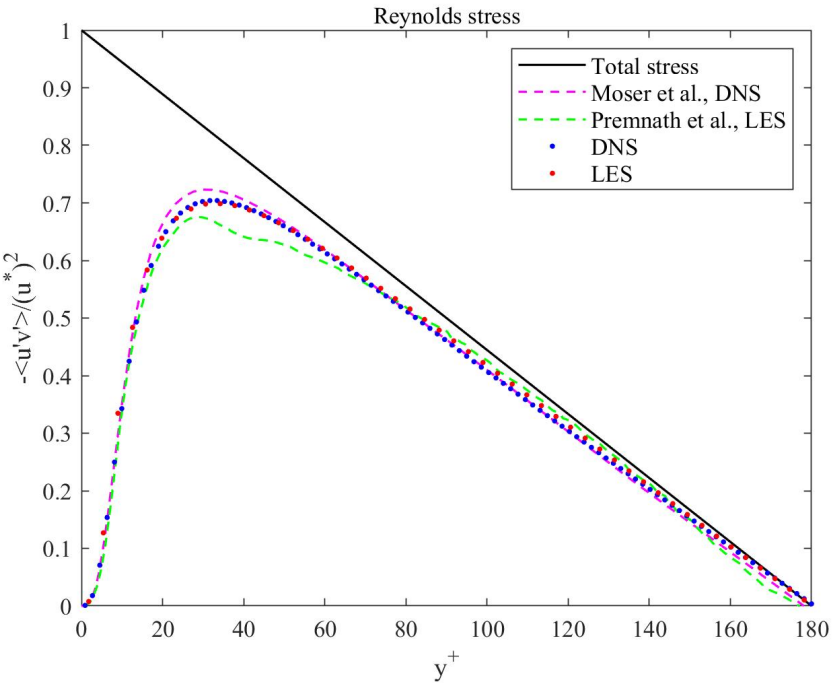

Figure 5 The mean turbulent Reynolds stress profiles normalized by u^{*2} in half of the channel. The black line represents the total stress.

Fig. 6 shows the mean root-mean-square velocity profiles of x, y and z components normalized by u^*. The normalized root-mean-square velocities of three components of turbulent flows can be described as

$$u_{rms}^{+} = \frac{u_{rms}}{u^{*}} \ (streamwise) \tag{23}$$

$$v_{rms}^{+} = \frac{v_{rms}}{u^{*}} \ (transverse) \tag{24}$$

$$w_{rms}^{+} = \frac{w_{rms}}{u^{*}} \ (spanwise) \tag{25}$$

The root-mean-square velocity signifies the standard deviation of the collection of "random" velocity fluctuations. A higher root-mean-square velocity indicates higher turbulence intensity. The LES results are essentially identical with the DNS results and Moser et al.'s data. In this case, the LES results of this study are much better than Premnath et al.'s data, showing the great accuracy and applicability of the LES method.

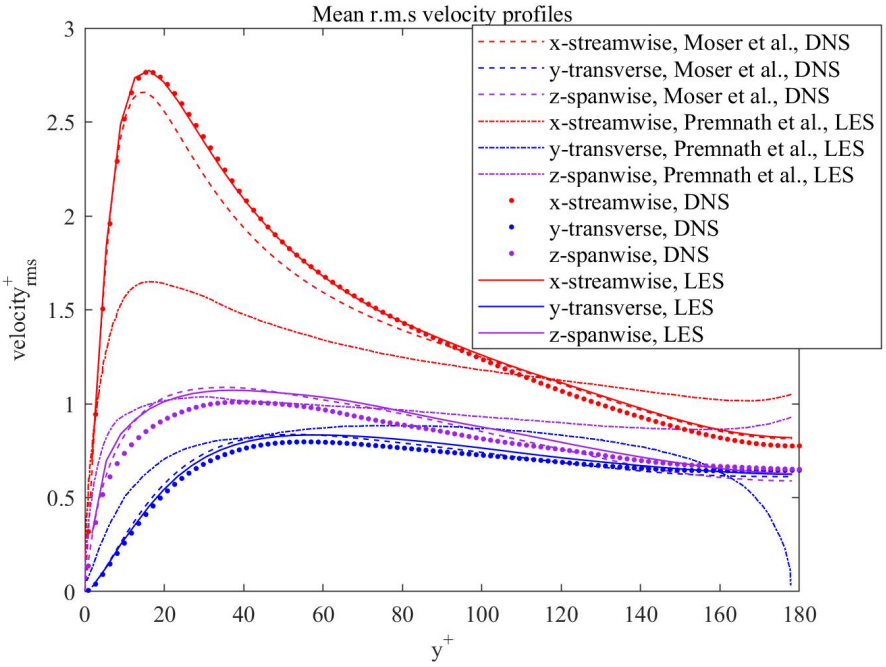

Figure 6 The normalized mean r.m.s velocity profiles in half of the channel from LES, DNS approaches and published data.

Fig. 7 shows the transverse (wall-normal) gradient of the streamwise velocity in

the transverse direction in half of the channel obtained from DNS and LES methods. The velocity gradient as well as the distance from the wall shown here is normalized as $u^+ = \frac{u}{u^*}$ and $y^+ = \frac{yu^*}{\nu}$. The largest velocity gradient happens in the regions near the wall, i.e. the viscous sublayer. As approaching the center of the channel, the velocity gradient decreases gradually. After reaching the logarithmic inertial layer, the velocity gradient becomes small and exactly 0 at the right center of the channel. Note that the velocity gradients of the first off-wall grid and the second off-wall grid of LES method are in a straight line, different from the DNS method, because of the use of the Musker wall model.

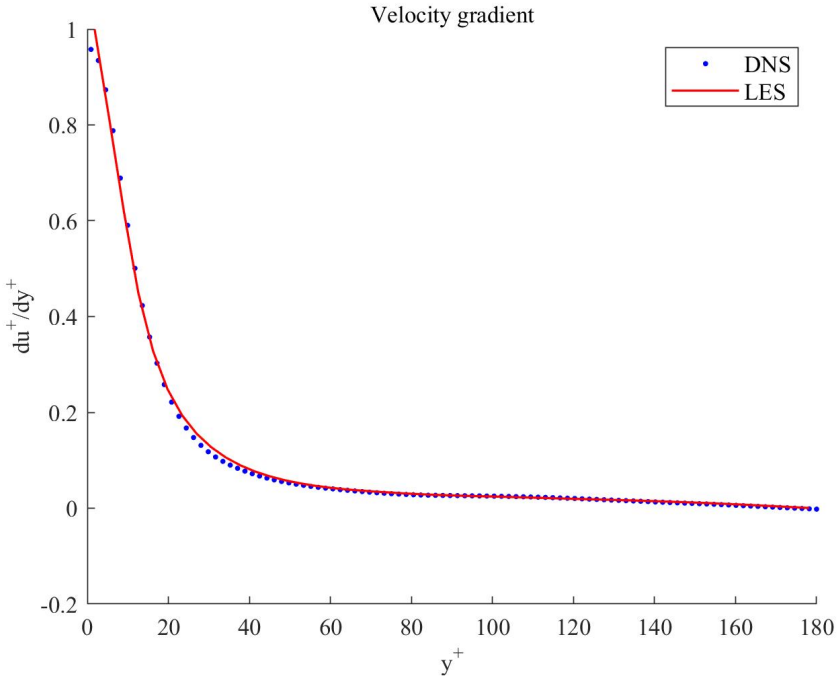

Figure 7 The streamwise velocity gradient in the wall-normal direction in half of the channel from LES, DNS approaches.

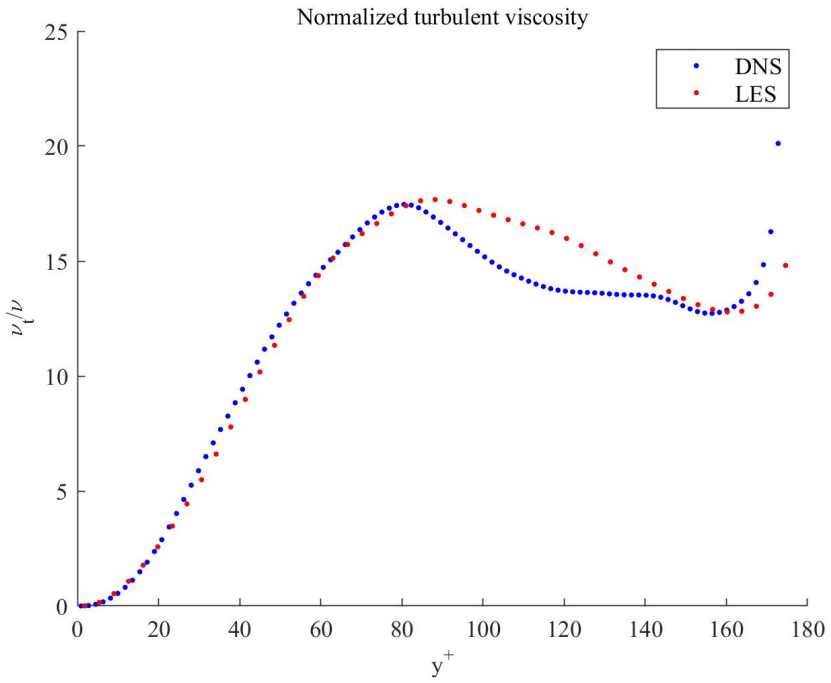

Figure 8 The turbulent viscosity normalized by molecular viscosity in half of the channel from LES, DNS approaches.

Fig. 8 shows the normalized turbulent viscosity in half of the channel from the DNS and LES approaches. The turbulent viscosity ν_t is normalized by molecular viscosity ν, which means that the turbulent viscosity is 15 times the molecular viscosity approximately. The two profiles are in reasonable agreement.

In summary, the accuracy and applicability of the LES approach are validated, by comparing the results with DNS method and the published data of Moser et al. and Premnath et al.

5. Conclusions

This study aims to develop and assess an advanced numerical method, combining the lattice Boltzmann method and the large-eddy simulation, for simulating turbulent flows more efficiently with fewer grid resolutions for practical engineering applications. In this research, the Smagorinsky sub-grid scale model and the Musker wall model are incorporated into the original DNS code utilizing LBM. To

validate this new approach, the LES method is implemented to simulate turbulent channel flow at $Re_\tau = 180$ and the results are compared with those from DNS and other researchers at the same Reynolds number. The LES uses only half the grid resolution of DNS. A non-uniform force field is applied to excite the turbulent flow. The mean flow velocity initially decreases rapidly due to the transfer of the kinetic energy from the mean flow to turbulent fluctuations, subsequently rebounding and reaching a stationary stage after normalized time $t^* = 38$.

As this study focuses on statistical data, the spanwise and streamwise data are averaged, emphasizing the variation of fluid properties in the transverse direction. The mean flow velocity profiles, mean turbulent Reynolds stress profiles, mean root-mean-square velocity profiles, the transverse gradient of the streamwise velocity, and normalized turbulent viscosity profiles are analyzed and compared. The LES method effectively captures the average velocity profile in the viscous sublayer and the logarithmic layer. The LES results show excellent agreement with the DNS results and the published data of Moser et al. and Premnath et al.

From the findings, it is evident that the LES approach holds the potential to simulate turbulent flows accurately and efficiently. The combination of LES method and wall model in LBM exhibits significant potential for further development. This approach can be applied to simulate turbulent flows with higher Reynolds numbers and even more complex flows, such as urban canopy flow, with future advancements.

References

[1] Sagaut P. Large eddy simulation for incompressible flows: an introduction[M]. Springer Science & Business Media, 2006.

[2] Launder B E, Spalding D B. Lectures in mathematical models of turbulence[J]. 1972.

[3] Bastin F, Lafon P, Candel S. Computation of jet mixing noise due to coherent structures: the plane jet case[J]. Journal of fluid mechanics, 1997, 335: 261-304.

[4] Vandromme D, Haminh H. The compressible mixing layer[J]. Turbulence and Coherent Structures: Selected Papers from "Turbulence 89: Organized Structures and Turbulence in Fluid Mechanics", Grenoble, 18–21 September 1989, 1991: 507-523.

[5] Smagorinsky J. General circulation experiments with the primitive equations[J]. Monthly weather review, 1963, 91(3): 99-164.

[6] Deardorff J W. A numerical study of three-dimensional turbulent channel flow at large Reynolds numbers[J]. Journal of Fluid Mechanics, 1970, 41(2): 453-480.

[7] Germano M, Piomelli U, Moin P, et al. A dynamic subgrid-scale eddy viscosity model[J]. Physics of Fluids A: Fluid Dynamics, 1991, 3(7): 1760-1765.

[8] Meneveau C, Lund T S, Cabot W H. A Lagrangian dynamic subgrid-scale model of turbulence[J]. Journal of fluid mechanics, 1996, 319: 353-385.

[9] Schumann U. Subgrid scale model for finite difference simulations of turbulent flows in plane channels and annuli[J]. Journal of computational physics, 1975, 18(4): 376-404.

[10] Musker A J. Explicit expression for the smooth wall velocity distribution in a turbulent boundary layer[J]. AIAA Journal, 1979, 17(6): 655-657.

[11] Schumann U. Subgrid scale model for finite difference simulations of turbulent flows in plane channels and annuli[J]. Journal of computational physics, 1975, 18(4): 376-404.

[12] Grötzbach G. Direct numerical and large eddy simulation of turbulent channel flows[J]. Encyclopedia of fluid mechanics, 1987, 6: 1337-1391.

[13] Shan X, Yuan X F, Chen H. Kinetic theory representation of hydrodynamics: a way beyond the Navier–Stokes equation[J]. Journal of Fluid Mechanics, 2006, 550: 413-441.

[14] Frapolli N, Chikatamarla S S, Karlin I V. Entropic lattice Boltzmann model for compressible flows[J]. Physical Review E, 2015, 92(6): 061301.

[15] Wang L P, Peng C, Guo Z, et al. Lattice Boltzmann simulation of particle-laden turbulent channel flow[J]. Computers & Fluids, 2016, 124: 226-236.

[16] Maeyama H, Imamura T, Osaka J, et al. Turbulent channel flow simulations using the lattice Boltzmann method with near-wall modeling on a non-body-fitted Cartesian grid[J]. Computers & Mathematics with Applications, 2021, 93: 20-31.

[17] Zhuo C, Zhong C. LES-based filter-matrix lattice Boltzmann model for simulating fully developed turbulent channel flow[J]. International Journal of Computational Fluid Dynamics, 2016, 30(7-10): 543-553.

[18] P.L. Bhatnagar, E.P. Gross, M. Krook, A model for collision processes in gases. I. Small amplitude processes in charged and neutral one-component systems, Phys. Rev. 94 (1954) 511–525, http://dx.doi.org/10.1103/PhysRev.94.511.

[19] Chai Z, Zhao T S. Effect of the forcing term in the multiple-relaxation-time lattice Boltzmann equation on the shear stress or the strain rate tensor[J]. Physical Review E, 2012, 86(1):

016705.
[20] He X, Luo L S. Lattice Boltzmann model for the incompressible Navier–Stokes equation[J]. Journal of statistical Physics, 1997, 88: 927-944.
[21] Kolmogorov A N. Local structure of turbulence in an incompressible viscous fluid at very high Reynolds numbers[J]. Soviet Physics Uspekhi, 1968, 10(6): 734.
[22] Guo Z, Shu C. Lattice Boltzmann method and its application in engineering[M]. World Scientific, 2013.
[23] Musker A J. Explicit expression for the smooth wall velocity distribution in a turbulent boundary layer[J]. AIAA Journal, 1979, 17(6): 655-657.
[24] Van Driest E R. On turbulent flow near a wall[J]. Journal of the aeronautical sciences, 1956, 23(11): 1007-1011.
[25] Nagib H M, Chauhan K A. Variations of von Kármán coefficient in canonical flows[J]. Physics of fluids, 2008, 20(10): 101518.
[26] Malaspinas O, Sagaut P. Wall model for large-eddy simulation based on the lattice Boltzmann method[J]. Journal of Computational Physics, 2014, 275: 25-40.
[27] Moser R D, Kim J, Mansour N N. Direct numerical simulation of turbulent channel flow up to Re τ= 590[J]. Physics of fluids, 1999, 11(4): 943-945.
[28] Premnath K N, Pattison M J, Banerjee S. Dynamic subgrid scale modeling of turbulent flows using lattice-Boltzmann method[J]. Physica A: Statistical Mechanics and its Applications, 2009, 388(13): 2640-2658.

Acknowledgement

First and foremost, I would like to convey my heartfelt gratitude to my research supervisor, Professor Lian-ping Wang, for his unwavering guidance and encouragement throughout my undergraduate studies and research endeavors, in addition to his patience, encouragement, and inspiration. His invaluable guidance has significantly aided me in both my research and decision-making processes. I am truly grateful to have such a distinguished mentor at the onset of my academic career.

My appreciation also extends to Dr. Hui Gao, currently an associate research professor at Southern University of Science and Technology, for his generous help in both my research and thesis preparation. He has graciously provided invaluable advice and guidance for me. Collaborating with Dr. Gao has been an exceptionally rewarding and efficient experience. I must acknowledge his innovative thinking and relentless efforts in spearheading research projects on large-eddy simulation. Without his support, I would not have had the opportunity to work through this project, let alone making some exciting discoveries.

Furthermore, I would like to extend my gratitude to my current and former laboratory colleagues at Southern University of Science and Technology, including, but not limited to, Zhiqiang Dong, Jun Lai, Hua Zhang, Zhuangzhuang Tian, Zehua Zhang, Chunyou Liu, Xiao Ji, and Lin Guo, for their generous help and support throughout my four-year undergraduate studies.